chemengineering

MDPI

Article

Vapor Pressure Mapping of Ionic Liquids and Low-Volatility Fluids Using Graded Isothermal Thermogravimetric Analysis

Sudhir Ravula [1,2], Nathaniel E. Larm [1], Mohammad A. Mottaleb [3], Mark P. Heitz [4,*] and Gary A. Baker [1,*]

1 Department of Chemistry, University of Missouri, Columbia, MO 65211, USA; sravula1@lsu.edu (S.R.); nelqmb@mail.missouri.edu (N.E.L.)
2 Department of Chemistry, Louisiana State University, Baton Rouge, LA 70803, USA
3 Department of Internal Medicine, Cardiovascular Medicine Division, University of Kentucky College of Medicine, Lexington, KY 40536, USA; m.a.mottaleb@uky.edu
4 Department of Chemistry and Biochemistry, The College at Brockport SUNY, Brockport, NY 14420, USA
* Correspondence: mheitz@brockport.edu (M.P.H.); bakergar@missouri.edu (G.A.B.); Tel.: +585-395-5586 (M.P.H.); +573-882-1811 (G.A.B.)

Received: 21 December 2018; Accepted: 17 April 2019; Published: 20 April 2019

Abstract: One of the hallmarks of ionic liquids (ILs) and a critical part of their sustainable implementation is their low volatility, although statements in this regard are frequently made in the absence of a critical evaluation. Although it is generally accepted that conventional ILs exhibit significantly reduced vapor pressures relative to common organic solvents, glib statements about ILs having zero volatility can no longer be abided, even if a concrete temperature-dependent vapor pressure, $P_{vap}(T)$, framework for placement of IL performance has not yet been established. In this communication, $P_{vap}(T)$ values of 30 illustrative low-volatility fluids—including representative imidazolium-, ammonium-, and pyrrolidinium-based aprotic ILs; examples of protic, polymeric, and di-cationic ILs; as well as deep eutectic solvents (DESs) and glycols—were determined using a simple, convenient, and reproducible isothermal thermogravimetric method. Guided by this "vapor pressure map", observed trends can be discussed in terms of anion basicity, cation geometry, alkane chain length, hydrogen bonding strength, and van der Waals forces, providing a context for the placement of theoretical and experimental vapor pressures gleaned in future IL and DES studies.

Keywords: ionic liquids; vapor pressure; thermogravimetric analysis; deep eutectic solvents

1. Introduction

Ionic liquids (ILs) are a class of molten salts that possess unusually low melting points (generally less than 373.15 K) and a reputation for exhibiting essentially no vapor pressure (P_{vap}), properties that distinguish them from conventional solvents [1,2]. In addition, ILs are considered to be designer solvents because their physicochemical properties can be tuned by selective combination of cation and anion chemical identities. Perhaps more than a million binary mixtures and over 10^{12} ternary mixtures are possible, generating a need to analyze the physicochemical properties of ILs and elucidate trends to predict these properties for other ion pair combinations [3]. One of the more attractive features of ILs is their negligible P_{vap}, a property which has provoked their application in catalysis, extraction, absorption, and chromatography [4,5]. While this property was once thought to be so low as to be inconsequential, it can actually be measured under reduced pressure and/or high temperatures [6–9]. In 2005, Rebelo et al. [6] were the first to estimate the P_{vap} and normal boiling temperature of ILs based on experimental surface tension and density. Later, Earle et al. [7] reported the vacuum

distillation of ILs using a Kugelrohr and sublimation apparatus at 473.15–573.15 K, with no signs of decomposition either in the distillate or residue. Both works showed that the P_{vap} of ILs can indeed be measured, which encouraged the study of their thermodynamic behavior (P_{vap}, enthalpy of vaporization ($\Delta_{vap}H$), distillation temperature, and boiling temperature) for a wide range of ILs using both experimental [10–14] and theoretical [15–18] methods. Rigorous determination of these properties could prove invaluable for gas-phase synthesis and purification of ILs, potentially allowing for IL distillation and alleviating long-standing issues regarding IL impurity.

Deep eutectic solvents (DESs) are an emerging class of liquids that are generally considered to be attractive alternatives to ILs due to similarities in their physicochemical properties [19,20] while being easier to prepare and purify, less expensive, less toxic, and more biodegradable and environmentally friendly. DESs should be more volatile at a given temperature because they contain molecular (non-ionic) components and rely instead on hydrogen bonding for component association, but to what extent is not well-known. Reports of efforts to measure P_{vap} and $\Delta_{vap}H$ for DESs are extremely rare [21,22], but of particular note and related to this study, Shahbaz et al. [23] measured the volatile nature of DES mixtures using a thermogravimetric analysis method between 343.15 and 393.15 K.

Numerous techniques, including the Knudsen method [10,11], temperature-programmed desorption line of sight mass spectrometry (LOMS) [17,24], high-temperature absorbance (UV) spectroscopy [25], quartz crystal microbalance (QCM) analysis [14,26], calorimetry [16,27], transpiration [16,28], and thermogravimetric analysis (TGA) [13,29,30], have been utilized to measure the free evaporation process of ILs as a function of temperature. Notably, the use of TGA is straightforward, reliable, and reproducible, requiring minimal sample size and time allocation while allowing for a wide temperature range analysis under controlled conditions. Luo et al. [13] were the first to use an isothermal gravimetric method to determine the $\Delta_{vap}H$ of 1-alkyl-3-methylimidazolium ($[C_nmIm^+]$) ILs (paired with $[Tf_2N^-]$ or $[beti^-]$ anions, where n is the number of carbons in the alkyl chain; see structures in Figure S1) for an accuracy of ±3 kJ·mol^{-1}. They observed two interesting outcomes: $\Delta_{vap}H$ values for $[C_nmIm][Tf_2N]$ were consistently ~5% higher than their $[beti^-]$ counterparts, and a methyl group at the C_2 position in $[C_nmIm^+]$ possesses a distinctly higher $\Delta_{vap}H$ value relative to an analog with the same side chain length and no methylated C_2.

A great deal of effort has been devoted to determining and understanding structure-property ($\Delta_{vap}H$) relationships for several series of ILs, although discrepancies still exist within these data. Recently, Deyko et al. [31] and Zaitsau et al. [32] analyzed the $\Delta_{vap}H$ for a series of pyrrolidinium- and pyridinium-based ILs using LOMS and QCM-TGA, respectively. However, as ILs become more extensively applied in evolving technologies (e.g., Li-ion batteries, solar energy conversion, waste recycling, cellulose processing), the glaring issue is that they cannot be designed based on their P_{vap} and $\Delta_{vap}H$ values. Therefore, a need exists to develop a simple method to measure or estimate the P_{vap} values of all classes of ILs at various temperatures.

We present a simple, straightforward, and reproducible TGA method to measure the P_{vap} of various ILs, DESs, and molecular solvents at various temperatures below their respective decomposition temperatures (T_{dcp}). A total of 30 low-volatility liquids were investigated, and their determined P_{vap} values were compared against those found in the literature. Structure-volatility trends are discussed in association with physiochemical properties, such as polarity scales (hydrogen-bond acidity (α), hydrogen-bond basicity (β), polarizability (π^*), $E_T(30)$), structural geometry, and distillation temperatures. These data will allow for the understanding and design of ILs and DESs with reduced vapor pressure in a host of applications.

2. Materials and Methods

2.1. Materials

All fluids investigated herein were either obtained commercially or were synthesized and purified in-house, as summarized in Table S1 of the Supplementary data. Purification was performed as specified

in the supplied references for each liquid, with an example ^{1}H-NMR spectrum for [C_4mIm][Tf_2N] provided in Figure S2. All fluids were dried under vacuum for at least 12 h at a temperature well below T_{dcp} prior to analysis. For instance, conventional ILs were dried at 343.15 K for 24 h.

2.2. Vapor Pressure Measurements

Thermogravimetric analysis was performed using either a TGA-Q50 V20.13 Build 39 (designated as TGA-1) or a Perkin Elmer TGA, Model 4000 (TGA-2). Sample weights were in the 10–80 mg range. A heating ramp of 10 °C·min^{-1} was used to bring samples from room temperature to their respective hold temperature. The isothermal gravimetric analysis was performed similarly to earlier work utilizing a 300 min hold period [13]. Samples were analyzed within a dry nitrogen stream at a flow rate of 60 mL·min^{-1} (TGA-1) or 20 mL·min^{-1} (TGA-2) to prevent sample oxidation. Uniform sample cross-sectional areas were maintained using platinum (TGA-1) or ceramic (TGA-2) crucibles. Four distinct analysis temperatures were selected for each sample based on the thermal stability shown in a scanning TGA experiment. Experimental isothermal temperatures were typically in the 100–160 (373.15–433.15 K) or 190–250 °C (463.15–523.15) range for ILs and in the 60–140 °C (333.15–413.15 K) regime for polyols and DESs. A fresh sample on a clean TGA pan (i.e., previously heated in air to 800 °C (1073.15 K) for 30 min in a Thermo Scientific™ Thermolyne™ benchtop muffle furnace, then allowed to cool to room temperature) was used for each temperature. Sigma Plot 11.0 software was used for statistical analysis and plotting.

2.3. Fluid Water Contents

As we demonstrated previously [13], disregarding the first 120 min of isothermal TGA data collection ensured that evaporation of minor traces of water did not contribute to the observed mass loss profiles. Indeed, the resulting thermograms were rigorously zero-order in mass loss and highly linear ($r^2 \geq 0.99$), consistent with clean evaporative loss of the fluid in question, with no discernible interference from water. The initial water contents (i.e., prior to the 120 min of in situ drying on the TGA instrument) for conventional hydrophobic, water-immiscible ILs (fluids #2, 6, 8–18, 21, and 30 in the Supplementary data) were in the range of 30–100 ppm, values that should be considered scrupulously dry [33]. The initial water contents for hydrophilic, water-miscible ILs (fluid #1, 3–5, 7, 19, and 20) fell in the 100–600 ppm range, and 500–2000 ppm for the protic IL propylammonium nitrate (PAN, #28) and the DESs, glycols, and polyols (fluid #22–27, 29, and 31). When considering the possible contribution from traces of water, it should be noted that water's vapor pressure at the temperatures analyzed (313.15–623.15 K) falls in the 103–107 Pa range, which is orders of magnitude higher than that of the tested liquids, in some cases being as much as four or five orders of magnitude higher at a particular temperature.

3. Results and Discussion

In this work, 30 liquids were either acquired commercially or synthesized in-house. Detailed information, including solvent names, structures, abbreviations, T_{dcp}, densities, viscosities, and thermal stabilities, are compiled in Figures S1 and S3, and Table S1. Gückel et al. [34,35] have extensively studied the P_{vap} of pesticides using an isothermal gravimetric method at ambient pressure and suggested that the logarithm of the evaporation rate (k) of a substance at a given temperature is linearly proportional to the logarithm of vapor pressure at this temperature:

$$\ln(P_{vap}) = a \ln(k) + b \quad (1)$$

where P_{vap} is the vapor pressure of a substance (bar) at a given temperature and k is the corresponding evaporation rate (%·min^{-1}). The coefficients (a and b) are dependent on the instrument, operational conditions (e.g., gas purge rate), and sample containment procedures [36]. This proportionality is reported to be independent of the sample and the temperature range [13,23,37,38]. Glycerol was

used as a reference compound to attain the instrument constants for our TGA instrument (TGA-1) because the P_{vap} data are well-established. Figure 1 illustrates the typical isothermal mass loss of glycerol under nitrogen purge, yielding linear curves (pseudo-zeroth-order) with $r^2 \geq 0.99$ (note that temperatures greater than 353.15 K produced more linear mass losses with $r^2 \geq 0.9998$). This linear relationship provides evidence that vaporization is the sole cause of mass loss in the absence of sample degradation or evolution of impurities. A range of holding temperatures was chosen to acquire instrument coefficients. Further, the evaporation rates of glycerol are comparable with repetitive measurements (Figure 1B) and consistent with those found in the literature [37]. Hereafter, mean evaporation rate values measured on TGA-1 were used to estimate P_{vap} data. Experiments were repeated on a different TGA instrument (denoted TGA-2), under similar conditions (see experimental section for details).

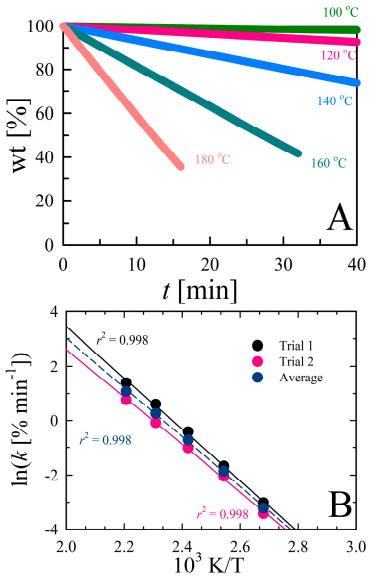

Figure 1. (**A**) Normalized mass loss curves for glycerol determined at various temperatures under nitrogen purge. (**B**) Comparison of temperature-dependent glycerol evaporation rates measured using isothermal gravimetry for two different trials. The average response for this particular apparatus (TGA-1) is denoted by the dashed profile.

Figure S4 and Table S2 provide the determined evaporation rates, suggesting that isothermal vaporization of glycerol is comparable between instruments. Figure S5 shows the P_{vap} data of glycerol obtained from the literature and the results correlate with each other, suggesting the reproducibility and consistency of the data. The standard glycerol P_{vap} data from the literature [37,39] and the evaporation rates measured in this work were plotted according to Equation (1). Figure 2 shows a linear correlation between the P_{vap} and rates of glycerol evaporation estimated using TGA-1 and -2, with $r^2 = 0.995$.

$$\text{TGA-1}: \ \ln\left(P_{vap}\right) = 1.07(\pm 0.02)\ln k - 4.88(\pm 0.04) \quad (2)$$

$$r^2 = 0.999, \ \text{SE} = \ 0.077$$

$$\text{TGA-2}: \ \ln\left(P_{vap}\right) = \ 1.04(\pm 0.05)\ln k - 4.35(\pm 0.15) \quad (3)$$

$$r^2 = 0.990, \ \text{SE} = 0.253$$

The instrument coefficients of Equation (1) for TGA-1 and TGA-2 are: $a = 1.14 \pm 0.03$ and 0.98 ± 0.02, and $b = -5.04 \pm 0.07$ and -4.47 ± 0.06, respectively. The a and b coefficients of the two instruments exhibit high precision and produced values within 8% of each other. Thus, we conservatively estimate that any calculated P_{vap} values will be reliable to within 10% if the instrument conditions remain

constant (e.g., crucible area, gas purge rate). By substituting the measured coefficients into Equation (1), the P_{vap} of any substance can be calculated on a per-instrument basis.

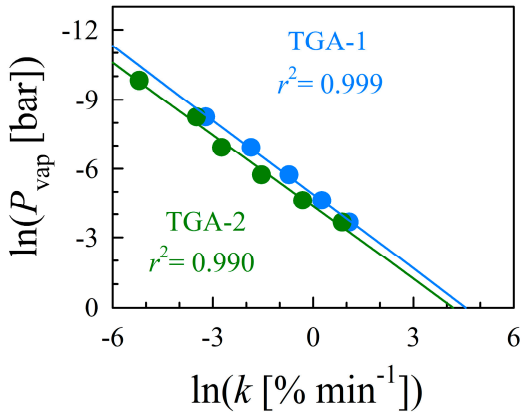

Figure 2. The linear relationship between the natural logs of both the evaporation rates of glycerol and their corresponding P_{vap} as reported in the literature [37,39]. The theoretical line is obtained by fitting the data to Equation (1) with r^2 = 0.995. Coefficients *a* and *b* represent the constants of Equation (1), which are dependent on the instrument and operational parameters.

3.1. Vapor Pressure Determination for [C$_4$mIm][Tf$_2$N]

Figure 3 illustrates the thermal stability and normalized time-dependent isothermal gravimetric analysis of [C$_4$mIm][Tf$_2$N]. The T_{dcp} (Table S1, entry 8) was determined by finding the temperature at which 10% mass loss was observed after initial solvent evaporation. Four distinct temperatures (463.15, 483.15, 503.15, and 523.15 K) below T_{dcp} were chosen for isothermal measurements. The first 120 min of the isotherm were discarded to eliminate solvent evaporation from our analysis, after which the remaining data were normalized with respect to mass to obtain a rigorously linear correlation (r^2 = 0.9999), with a slope that represents the evaporation rate for [C$_4$mIm][Tf$_2$N] at the respective temperature. Since TGA-1 was used for these experiments, Equation (2) was used to predict each corresponding P_{vap} (i.e., 0.1497, 0.2523, 0.9834, and 2.0647 Pa at 463.15, 483.15, 503.15, and 523.15 K, respectively). The thermal stabilities of 29 other liquids were measured in an analogous manner (Figure S3), isothermal gravimetric analysis temperatures were chosen accordingly, and their respective P_{vap} values were calculated and are tabulated in Table S3.

As seen in Table S3 and Figure 4, the P_{vap} values for ILs are in the range of 1.4×10^{-3} to 26.80 Pa at 373.15–523.15 K. The P_{vap} for [C$_4$mIm][Tf$_2$N] and [C$_6$mIm][Tf$_2$N] (Table S3, entries 8 and 9, respectively) have been studied using a variety of techniques and reported [10,11,26,40]. Several of these literature values are plotted with the P_{vap} values determined here to facilitate a more thorough assessment of our data (Figure S6A). The plot suggests that our vapor pressure results are in reasonably good agreement with the literature data, in particular with Brunetti et al. [40] and Rocha et al. [26]. However, the P_{vap} value obtained by Aschenbrenner et al. [29] for [C$_4$mIm][Tf$_2$N] at 393.15 K (1.2 Pa) is several orders of magnitude greater than our P_{vap} under similar conditions (2.029×10^{-3} Pa), despite using a similar TGA instrument. As our data closely matches literature data, we suggest that this discrepancy may be attributed to either the presence of impurities or solvent in their IL or the significantly brief evaporation period that they examined (10 min). In general, the evaporation rates (and therefore P_{vap}) for ILs decrease as the alkyl chain lengthens. This is due to the non-electrostatic interactions (i.e., van der Waals force) outweighing the electrostatic interactions (Coulombic force) because of efficient packing of alkyl chains and increased molecular weight, which results in greater electron density for polarization [12]. However, the volatility of [C$_6$mIm][Tf$_2$N] is indistinguishable from [C$_4$mIm][Tf$_2$N] (a finding that is consistent with those of Zaitsau et al. [11], Rocha et al. [26], and Rebelo et al. [6]), see Figure S6B, so this effect appears to be insignificant within the experimental temperature range for a two hydrocarbon difference.

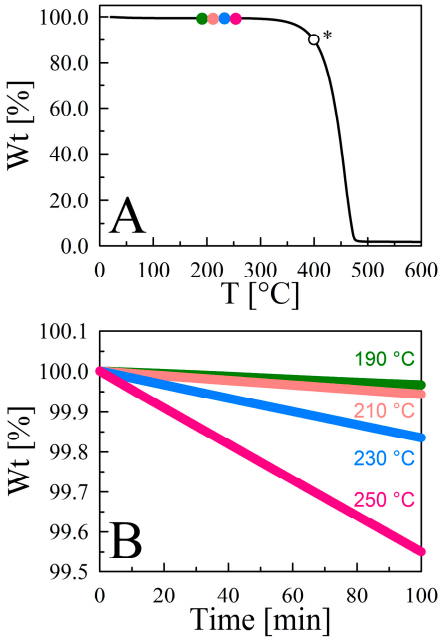

Figure 3. (**A**) Thermal stability of $[C_4mIm][Tf_2N]$ under nitrogen purge at a constant flow rate of 60 mL·min^{-1} from room temperature to 600 °C (873.15 K) at a heating rate of 10 °C·min^{-1}. The color of the symbols on the thermograms in panel A corresponds to the isothermal gravimetric weight loss curves in the lower panel. The open symbol marked * denotes the T_{dcp} (672.65 K) for this sample. (**B**) A normalized magnification showing the rigorously linear ($r^2 \geq 0.9999$) evaporation curves of $[C_4mIm][Tf_2N]$ at different temperatures.

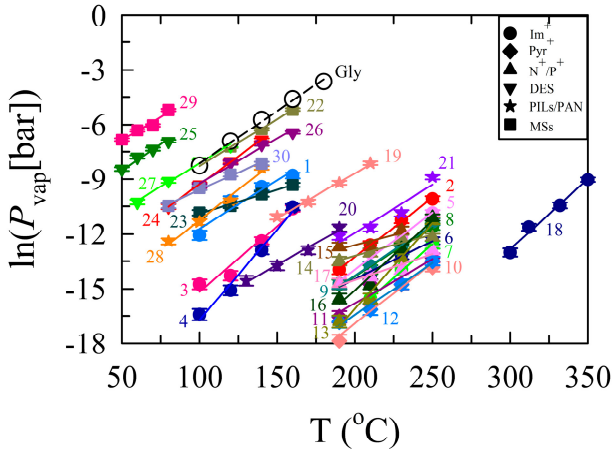

Figure 4. A map illustrating isothermal-gravimetry-determined temperature-dependent vapor pressure for representative ionic liquids (ILs), deep eutectic solvents (DESs), and miscellaneous low-volatility fluids. The individual solvents are identified numerically corresponding to the entries of Table S3 in the Supplementary Information. The solid lines connecting experimental values for a given liquid denote linear regression fits for vapor pressure data and are shown primarily to guide the eye. Legend abbreviations: Im+: imidazolium; Pyr+: pyrrolidinium; N^+/P^+: ammonium/phosphonium; PILs/PAN: polyionic liquids/propylammonium nitrate; MSs: molecular solvents. 1: $[C_2mIm][EtSO_4]$; 2: $[C_2mIm][beti]$; 3: $[C_4mIm][Br]$; 4: $[C_4mIm][dca]$; 5: $[C_4mIm][BF_4]$; 6: $[C_4mIm][PF_6]$; 7: $[C_4mIm][TfO]$; 8: $[C_4mIm][Tf_2N]$; 9: $[C_6mIm][Tf_2N]$; 10: $[C_3mPy][Tf_2N]$; 11: $[C_4mPy][Tf_2N]$; 12: $[C_6mPy][Tf_2N]$; 13: $[N_{ip311}][Tf_2N]$; 14: $[N_{6111}][Tf_2N]$; 15: $[N_{8111}][Tf_2N]$; 16: $[N_{8881}][Tf_2N]$; 17: $[P_{14,666}][Tf_2N]$; 18: $[C_3(C_1Im)_2]$ $[Tf_2N]_2$; 19: p([VBBIm][Cl]); 20: p([VBIm][Br]); 21: p([VBIm][Tf_2N]); 22: PEG 200; 23: PEG 600; 24: Reline; 25: Ethaline; 26: Glyceline; 27: Bu_4NBr:Im; 28: PAN; 29: Triglyme; 30:[Li(trigly)][Tf_2N]; Gly: Glycerol.

3.2. Effect of the Anion on IL Vapor Pressure

The size, shape, and nucleophilicity of the anions in ILs play a crucial role in determining the intermolecular forces that exist between the ions in the liquid phase, including ion–ion interactions, hydrogen bonding, polarizability, and van der Waals forces. However, very recently, Tokuda et al. [41,42] reported that the *ab initio* molecular orbital calculations of cation–anion interaction energies in [C_2mIm]-based ILs were −85.2, −82.6, −78.8, and −78.4 kcal·mol^{-1} for [BF4$^-$], [TfO$^-$], [Tf_2N^-], and [PF_6^-], respectively. These interaction energies clearly indicate that [C_4mIm^+] is more interactive with [BF_4^-] than [PF_6^-], therefore exhibiting a higher P_{vap}. In contrast, ILs involving [Tf_2N^-] vaporize more readily than those with [TfO$^-$] at all temperatures even though the interactive energy and basicity values of [Tf_2N^-] are lower than those of the [TfO$^-$] anion. This is likely caused by the slow diffusion of triflate salts due to high solution viscosity [43]. Additionally, this trend coincides with distillation work reported by Earle et al. [7] and Widegren et al. [12]. As a result, the observed vaporization trend for ILs with a similar cation and different anions is as follows: Br^- > [dca$^-$] > [BF_4^-] > [Tf_2N^-] > [PF_6^-] > [TfO$^-$]. Figure S7 displays a comparison between the present results and literature data [16,44] for [C_4mIm][PF_6] and [C_4mIm][dca].

3.3. Effect of the Cation on IL Vapor Pressure

Interestingly, the P_{vap} values of pyrrolidinium- and ammonium-based [Tf_2N^-] ILs (Table S3, entries 10–17) are less than those of the [C_nmIm][Tf_2N] IL series [12]. We attribute this to the planar geometry of [Im^+], which bistriflamide can effectively approach and form a stable ion pair reinforced through hydrogen bonding. The tetrahedral geometries of [Py^+] and [R_4N^+] complicate this interaction [12]. Therefore, the structure-volatility series determined in this study for different cation classes at 523.15 K is [C_6mIm^+] > [$N_{6111}{}^+$] > [C_4mPy^+]. Our results are in agreement with the solvatochromic polarity parameters of ILs and the experiments conducted in other groups, signifying that the aromatic compounds are more volatile than the non-aromatic compounds due to geometry [12,41,42,45].

In the case of [N_{ip311}][Tf_2N], the low-temperature P_{vap} is much lower than those of other long-chain alkyl groups, likely because the branched alkyl group influences the charge on the center and isolates the anion. Further, [$P_{14,666}$][Tf_2N] exhibits a lower P_{vap} at higher temperatures when compared to [N_{8881}][Tf_2N] and [$C_3(C_1Im)_2$][Tf_2N]$_2$ (Table S3, entries 17, 16, and 18, respectively). This decrease in volatility with increased alkyl chain length is attributed to the potential for longer-chain alkyl groups to pack more efficiently, resulting in increasing van der Waals interactions that ultimately outweigh the decreasing Coulombic interactions to decrease volatility [12]. Further, the di-cationic [$C_3(C_1Im)_2$][Tf_2N]$_2$ has a much lower P_{vap} result when compared to similar mono-cationic [$C_n$mim][Tf_2N] ILs, likely because the di-cationic species requires more energy to vaporize one mole of the neutral ion pair than an equivalent one mole of mono-cationic IL [44].

3.4. Vapor Pressure of Polyols

PEG 200 and triglyme (and the other polyol derivatives to a lesser extent) exhibited the highest P_{vap} values of any liquid tested in Figure 4 and Table S3. This finding is attributed to their lower molecular weights. The P_{vap} value found on a chemical database [46] for triglyme at 293.15 K is 0.12 kPa compared to the extrapolated P_{vap} (~0.02 kPa) in this study. As the database did not provide any explicit experimental details, we believe that our measurements are within the range of uncertainties. In addition, when comparing the P_{vap} of triglyme to its IL analog [Li(trigly)][Tf_2N] (Table S3, entry 30), we noted that the addition of Li^+ and [Tf_2N^-] provides strong Coulombic interactions, increasing the ionic character and density of the solvent while simultaneously decreasing the observed P_{vap} by over 2 orders of magnitude at 353.15 K [47]. Notably, this striking change in P_{vap} provides fundamental insight into the consequences with regard to solvent physicochemical properties of turning glymes into complex ions, a finding that may not be possible to correlate with other similar systems (e.g., crown ethers). PEG 600 (Table S3, entry 23) exhibits a similar decrease in P_{vap} when compared to PEG 200

due to an increase in molecular weight through the extension of the PEG chain [47]. Similar to what was observed previously, the P_{vap} values measured by Aschenbrenner et al. [29] for PEG 200 and PEG 600 at 368.15 K are 9.9 and 0.2 Pa, respectively, which are 2–8 times lower than our estimated values (19.86, and 1.77 Pa, respectively).

3.5. Vapor Pressure of DESs

We note that, strictly speaking, it is not currently possible to satisfactorily determine the vapor pressure for a deep eutectic solvent, given the lack of knowledge about the relative vapor pressures of the components when mixed and the possible evolution of component volatility during extensive evaporation. That is to say, estimating P_{vap} values for a DES system is complicated by the fact that DESs comprise two or more components (most typically, this means a salt pair plus a neutral hydrogen bond donor species) interacting via dynamic hydrogen bonding and it is not possible, by evaporation alone, to assert the nature of the volatile fraction. Whereas ion pairs are often assumed to be predominantly lost during ionic liquid evaporation a priori (and computational evidence exists to support this) [48], the neutral species is likely to display relatively higher volatility in the DES, complicating matters. Thus, any pronounced mass loss for a DES system likely corresponds to a change in the composition of the components over time. Having stated these caveats, we include representative DES vapor pressure data alongside our other studies for reasons of operational utility, as they still guide useful temperature regimes of application. That is, despite not representing rigorous vapor pressures for the reasons just outlined, we include DES vapor pressure values derived from thermogravimetric analysis to place them in useful context with values displayed by ionic liquids and other molecular solvents, with the understanding that they represent "apparent" P_{vap} values. Moreover, despite these stated limitations, P_{vap} values have in fact already been reported for typical DESs.

Table S3 and Figure 4 display the P_{vap} of four DES mixtures (entries 24–27), which fall in the range of 2.12–161.95 Pa at 313.15–433.15 K. These values are lower than their individual components due to strong intermolecular hydrogen bonding interactions between the hydrogen bond donator and a quaternary ammonium salt (choline chloride) in the mixtures. For instance, glyceline (Table S3, entry 26) possesses vapor pressures of 6.97 Pa at 373.15 K and 161.9 Pa at 433.15 K, which makes it 3.7–6.0 times less volatile than glycerol (P_{vap} = 26 and 980 Pa) [39] at the respective temperatures. The structure-volatility series for the DES mixtures containing choline chloride but with different hydrogen bond donors is ethaline > reline > glyceline (most to least volatile), emphasizing that ethaline is one of the most volatile DESs. This trend agrees with solvent polarity ($E_T(30)$ and α) values reported in the literature and TGA experiments conducted by Shahbaz et al. [23,49]. Figure S8 shows the temperature dependence of measured values against the Shahbaz data for reline and glyceline. The glyceline P_{vap} determined here coincides with their data, while we observe higher values for reline in our study.

3.6. Vapor Pressures of Protic ILs

Protic ILs are a subset of ILs that possess properties similar to those of typical ILs [50]. Of particular note, ethylammonium nitrate (EAN) and to a lesser extent propylammonium nitrate (PAN) have been widely studied, as EAN is regarded as the first truly room temperature ionic liquid to have been discovered [50,51]. Figure S9 presents the P_{vap} values of PAN (this work) and EAN (as measured by Emel'yanenko et al. [52]) as a function of temperature, indicating the slightly more volatile nature of PAN when compared to EAN. This difference in volatility is attributed to the intermolecular hydrogen bonding interactions between the ions (+NH•••O–). As the alkyl chain lengthens, the average distance between ions increases, making weaker hydrogen bonds that result in increased P_{vap} [53]. In addition, the exponential rise in vaporization at 413 K indicates acid-base proton transfer to form neutral molecules. Nevertheless, reasonable agreement was observed between these two data sets. Moreover, the vapor values of PAN and EAN are much lower than those of DESs, PEG 200, and molecular solvents, promoting the use of protic ILs as electrolytes for batteries and fuel cells.

4. Conclusions

In summary, we have presented a simple and efficient isothermal TGA method for rapid screening of the P_{vap} values for liquid compounds possessing extremely low volatilities. The measured evaporation rates of a reference sample (glycerol) were repeatable and reproducible, allowing for the determination of instrument constants for use in our study. The P_{vap} was estimated for 30 liquids, and when possible, validated against literature values. We found that triglyme and PEG 200 are more volatile than longer-chain analogs, followed (in general) by DESs, protic ILs, polymeric ILs, imidazolium-, ammonium-, and pyrrolidinium-based Tf_2N ILs, and finally di-cationic ILs. However, solvent volatility was found to be dependent on the specific IL cation–anion combination. Our results show that the P_{vap} of related fluids can be estimated within 10% uncertainty. Our method can easily be applied to calculate instrument constants for the determination of P_{vap} values in other laboratories. Overall, this method was successfully used to analyze the vaporization of substances once thought and claimed to have zero vapor pressure and provides valuable information towards the design of future ILs and other low-volatility solvents.

Supplementary Materials: The following are available online at http://www.mdpi.com/2305-7084/3/2/42/s1, Table S1: Names, abbreviations, sources, molecular weights, decomposition temperatures, densities, viscosities, and typical water contents of scrupulously dry ionic liquids and other solvents studied; Table S2: The experimental evaporation rates of glycerol measured on two different commercial TGA instruments and the vapor pressures values taken from the literature; Table S3: Vapor pressure summary of ILs, DESs, and miscellaneous low-volatility conventional solvents at various temperatures; Figure S1: Summary of cations, anions, DESs, and other solvents studied and their abbreviations (R = alkyl group); Figure S2: Representative ^{1}H-NMR spectrum for $[C_4mIm][Tf_2N]$ using deuterated acetone as the solvent. Peaks are assigned numerically beside the molecule; Figure S3: Thermal stabilities of 30 liquids. (A) $[C_4mIm]$-based ILs with different anionic structures (5: $[C_4mIm][BF_4]$; 6: $[C_4mIm][PF_6]$; 7: $[C_4mIm][TfO]$; 8: $[C_4mIm][Tf_2N]$; 9: $[C_6mIm][Tf_2N]$); (B) ammonium-, and pyrrolidinium-based Tf_2N ILs; (C) PEGs, dicationic ILs, $[P_{14,6,6,6}][Tf_2N]$, and polymeric ILs; (D) protic IL, triglyme, and DESs; Figure S4: Comparison of experimental evaporation rates of glycerol measured on two commercial instruments (TGA-1 and TGA-2) at various temperatures. The evaporation rate of glycerol from both instruments are comparable with each other and are used to estimate the instrument coefficients (*a* and *b*); Figure S5: P_{vap} values of pure glycerol obtained from the literature (blue: ref [24], dark green: ref. [25], and black: ref. [26]. All P_{vap} data obtained from different studies at different temperatures correlate with each other, suggesting the P_{vap} values are consistent and reliable. P_{vap} values used in this study originate from ref. [24]; Figure S6: Correlation between present and literature P_{vap} values with respect to temperature. (Upper) $[C_4mim][Tf_2N]$ (Zaitsau et al. [27], Rocha et al. [28], Aschenbrenner et al. [29], and Brunetti et al. [30]). (Lower) $[C_6mim][Tf_2N]$ (Zaitsau et al. [27] and Rocha et al. [28]); Figure S7: Comparison of P_{vap} results with literature data as function of temperature. (A) $[C_4mim][PF_6]$ (Zaitsau et al. [31]), (B) $[C_4mim][dca]$ (Emel'yanenko et al. [32]); Figure S8: P_{vap} results of glyceline (circles) and reline (rhombus) DESs mixtures in comparison with Shahbaz et al. [34]. This study (blue) and Shahbaz et al. (green) were measured using TGA. Inset shows the values of reline measured by Shahbaz et al.; Figure S9: P_{vap} plot of PAN (as measured in this study) and EAN (as measured by Emel'yanenko et al. [35]) as a function of temperature.

Author Contributions: Conceptualization, G.A.B.; Data curation, S.R., N.E.L. and M.A.M.; Formal analysis, S.R., N.E.L. and M.A.M.; Funding acquisition, G.A.B.; Project administration, M.P.H. and G.A.B.; Supervision, G.A.B.; Validation, S.R., M.P.H. and G.A.B.; Writing—original draft, S.R.; Writing—review & editing, N.E.L., M.P.H. and G.A.B.

Funding: The current research was partially supported by a Research Council grant from the University of Missouri (G.A.B.) and by the Research Corporation for Science Advancement (G.A.B.).

Conflicts of Interest: The authors declare no conflict of interest. The funders had no role in the design of the study; in the collection, analyses, or interpretation of data; in the writing of the manuscript, or in the decision to publish the results.

References

1. Baker, G.A.; Baker, S.N.; Pandey, S.; Bright, F.V. An Analytical View of Ionic Liquids. *Analyst* **2005**, *130*, 800–808. [CrossRef] [PubMed]
2. Castner, E.W., Jr.; Margulis, C.J.; Maroncelli, M.; Wishart, J.F. Ionic Liquids: Structure and Photochemical Reactions. *Annu. Rev. Phys. Chem.* **2011**, *62*, 85–105. [CrossRef] [PubMed]
3. Rogers, R.D.; Seddon, K.R. Ionic Liquids–Solvents of the Future? *Science* **2003**, *302*, 792–793. [CrossRef] [PubMed]
4. Wishart, J.F. Energy Applications of Ionic Liquids. *Energy Environ. Sci.* **2009**, *2*, 956–961. [CrossRef]

5. Tang, S.; Baker, G.A.; Zhao, H. Ether- and Alcohol-Functionalized Task-Specific Ionic Liquids: Attractive Properties and Applications. *Chem. Soc. Rev.* **2012**, *41*, 4030–4066. [PubMed]
6. Rebelo, L.P.N.; Canongia Lopes, J.N.; Esperança, J.M.S.S.; Filipe, E. On the Critical Temperature, Normal Boiling Point, and Vapor Pressure of Ionic Liquids. *J. Phys. Chem. B* **2005**, *109*, 6040–6043. [CrossRef]
7. Earle, M.J.; Esperanca, J.M.S.S.; Gilea, M.A.; Canongia Lopes, J.N.; Rebelo, L.P.N.; Magee, J.W.; Seddon, K.R.; Widegren, J.A. The Distillation and Volatility of Ionic Liquids. *Nature* **2006**, *439*, 831–834. [CrossRef]
8. Esperança, J.M.S.S.; Canongia Lopes, J.N.; Tariq, M.; Santos, L.M.N.B.F.; Magee, J.W.; Rebelo, L.P.N. Volatility of Aprotic Ionic Liquids—A Review. *J. Chem. Eng. Data* **2010**, *55*, 3–12. [CrossRef]
9. Ludwig, R.; Kragl, U. Do We Understand the Volatility of Ionic Liquids? *Angew. Chem. Int. Ed.* **2007**, *46*, 6582–6584. [CrossRef]
10. Paulechka, Y.U.; Zaitsau, D.H.; Kabo, G.J.; Strechan, A.A. Vapor Pressure and Thermal Stability of Ionic Liquid 1-Butyl-3-methylimidazolium Bis(trifluoromethylsulfonyl)amide. *Thermochim. Acta* **2005**, *439*, 158–160. [CrossRef]
11. Zaitsau, D.H.; Kabo, G.J.; Strechan, A.A.; Paulechka, Y.U.; Tschersich, A.; Verevkin, S.P.; Heintz, A. Experimental Vapor Pressures of 1-Alkyl-3-methylimidazolium Bis(trifluoromethylsulfonyl)imides and a Correlation Scheme for Estimation of Vaporization Enthalpies of Ionic Liquids. *J. Phys. Chem. A* **2006**, *110*, 7303–7306. [CrossRef]
12. Widegren, J.A.; Wang, Y.-M.; Henderson, W.A.; Magee, J.W. Relative Volatilities of Ionic Liquids by Vacuum Distillation of Mixtures. *J. Phys. Chem. B* **2007**, *111*, 8959–8964. [CrossRef]
13. Luo, H.; Baker, G.A.; Dai, S. Isothermogravimetric Determination of the Enthalpies of Vaporization of 1-Alkyl-3-methylimidazolium Ionic Liquids. *J. Phys. Chem. B* **2008**, *112*, 10077–10081. [CrossRef] [PubMed]
14. Verevkin, S.P.; Zaitsau, D.H.; Emelyanenko, V.N.; Heintz, A. A New Method for the Determination of Vaporization Enthalpies of Ionic Liquids at Low Temperatures. *J. Phys. Chem. B* **2011**, *115*, 12889–12895. [CrossRef]
15. Ludwig, R. Thermodynamic Properties of Ionic Liquids-A Cluster Approach. *Phys. Chem. Chem. Phys.* **2008**, *10*, 4333–4339. [CrossRef] [PubMed]
16. Emel'yanenko, V.N.; Verevkin, S.P.; Heintz, A. The Gaseous Enthalpy of Formation of the Ionic Liquid 1-Butyl-3-methylimidazolium Dicyanamide from Combustion Calorimetry, Vapor Pressure Measurements, and Ab Initio Calculations. *J. Am. Chem. Soc.* **2007**, *129*, 3930–3937. [CrossRef] [PubMed]
17. Armstrong, J.P.; Hurst, C.; Jones, R.G.; Licence, P.; Lovelock, K.R.J.; Satterley, C.J.; Villar-Garcia, I.J. Vapourisation of Ionic Liquids. *Phys. Chem. Chem. Phys.* **2007**, *9*, 982–990. [CrossRef] [PubMed]
18. Dong, K.; Zhao, L.; Wang, Q.; Song, Y.; Zhang, S. Are Ionic Liquids Pairwise in Gas Phase? A Cluster Approach and In situ IR Study. *Phys. Chem. Chem. Phys.* **2013**, *15*, 6034–6040. [CrossRef]
19. Sze, L.L.; Pandey, S.; Ravula, S.; Pandey, S.; Zhao, H.; Baker, G.A.; Baker, S.N. Ternary Deep Eutectic Solvents Tasked for Carbon Dioxide Capture. *ACS Sustain. Chem. Eng.* **2014**, *2*, 2117–2123. [CrossRef]
20. Wagle, D.V.; Zhao, H.; Baker, G.A. Deep Eutectic Solvents: Sustainable Media for Nanoscale and Functional Materials. *Acc. Chem. Res.* **2014**, *47*, 2299–2308. [CrossRef]
21. Wu, S.-H.; Caparanga, A.R.; Leron, R.B.; Li, M.-H. Vapor Pressure of Aqueous Choline Chloride-Based Deep Eutectic Solvents (ethaline, glyceline, maline and reline) at 30–70 °C. *Thermochim. Acta* **2012**, *544*, 1–5. [CrossRef]
22. Boisset, A.; Jacquemin, J.; Anouti, M. Physical Properties of a New Deep Eutectic Solvent Based on Lithium Bis[(trifluoromethyl)sulfonyl]imide and N-methylacetamide as Superionic Suitable Electrolyte for Lithium Ion Batteries and Electric Double Layer Capacitors. *Electrochim. Acta* **2013**, *102*, 120–126. [CrossRef]
23. Shahbaz, K.; Mjalli, F.S.; Vakili-Nezhaad, G.; AlNashef, I.M.; Asadov, A.; Farid, M.M. Thermogravimetric Measurement of Deep Eutectic Solvents Vapor Pressure. *J. Mol. Liq.* **2016**, *222*, 61–66. [CrossRef]
24. Deyko, A.; Hessey, S.G.; Licence, P.; Chernikova, E.A.; Krasovskiy, V.G.; Kustov, L.M.; Jones, R.G. The Enthalpies of Vaporisation of Ionic Liquids: New Measurements and Predictions. *Phys. Chem. Chem. Phys.* **2012**, *14*, 3181–3193. [CrossRef]
25. Wang, C.; Luo, H.; Li, H.; Dai, S. Direct UV-Spectroscopic Measurement of Selected Ionic-Liquid Vapors. *Phys. Chem. Chem. Phys.* **2010**, *12*, 7246–7250. [CrossRef]

26. Rocha, M.A.A.; Lima, C.F.R.A.C.; Gomes, L.R.; Schröder, B.; Coutinho, J.A.P.; Marrucho, I.M.; Esperança, J.M.S.S.; Rebelo, L.P.N.; Shimizu, K.; Lopes, J.N.C.; et al. High-Accuracy Vapor Pressure Data of the Extended $[C_nC_1im][NTf_2]$ Ionic Liquid Series: Trend Changes and Structural Shifts. *J. Phys. Chem. B* **2011**, *115*, 10919–10926. [CrossRef]
27. Santos, L.M.N.B.F.; Canongia Lopes, J.N.; Coutinho, J.A.P.; Esperança, J.M.S.S.; Gomes, L.R.; Marrucho, I.M.; Rebelo, L.P.N. Ionic Liquids: First Direct Determination of their Cohesive Energy. *J. Am. Chem. Soc.* **2007**, *129*, 284–285. [CrossRef] [PubMed]
28. Verevkin, S.P.; Zaitseva, K.V.; Stanton, A.D.; Hindman, M.S.; Irvin, A.C.; Bara, J.E. Building Blocks for Ionic Liquids: Vapor Pressures and Vaporization Enthalpies of N-Functionalized Imidazoles with Branched and Cycloalkyl Substituents. *Ind. Eng. Chem. Res.* **2015**, *54*, 9850–9856. [CrossRef]
29. Aschenbrenner, O.; Supasitmongkol, S.; Taylor, M.; Styring, P. Measurement of Vapour Pressures of Ionic Liquids and Other Low Vapour Pressure Solvents. *Green Chem.* **2009**, *11*, 1217–1221. [CrossRef]
30. Verevkin, S.P.; Ralys, R.V.; Zaitsau, D.H.; Emel'yanenko, V.N.; Schick, C. Express Thermo-Gravimetric Method for the Vaporization Enthalpies Appraisal for Very Low Volatile Molecular and Ionic Compounds. *Thermochim. Acta* **2012**, *538*, 55–62. [CrossRef]
31. Deyko, A.; Lovelock, K.R.J.; Corfield, J.-A.; Taylor, A.W.; Gooden, P.N.; Villar-Garcia, I.J.; Licence, P.; Jones, R.G.; Krasovskiy, V.G.; Chernikova, E.A.; et al. Measuring and Predicting $\Delta vapH_{298}$ Values of Ionic Liquids. *Phys. Chem. Chem. Phys.* **2009**, *11*, 8544–8555. [CrossRef]
32. Zaitsau, D.H.; Yermalayeu, A.V.; Emel'yanenko, V.N.; Heintz, A.; Verevkin, S.P.; Schick, C.; Berdzinski, S.; Strehmel, V. Structure–property Relationships in ILs: Vaporization Enthalpies of Pyrrolidinium Based Ionic Liquids. *J. Mol. Liq.* **2014**, *192*, 171–176. [CrossRef]
33. Jin, H.; O'Hare, B.; Dong, J.; Arzhantsev, S.; Baker, G.A.; Wishart, J.F.; Benesi, A.J.; Maroncelli, M. Physical Properties of Ionic Liquids Consisting of the 1-Butyl-3-Methylimidazolium Cation with Various Anions and the Bis(trifluoromethylsulfonyl)imide Anion with Various Cations. *J. Phys. Chem. B* **2008**, *112*, 81–92. [CrossRef]
34. Gückel, W.; Kästel, R.; Kröhl, T.; Parg, A. Methods for Determining the Vapour Pressure of Active Ingredients Used in Crop Protection. Part IV. An Improved Thermogravimetric Determination Based on Evaporation Rate. *Pestic. Sci.* **1995**, *45*, 27–31. [CrossRef]
35. Gückel, W.; Kästel, R.; Lewerenz, J.; Synnatschke, G. A Method for Determining the Volatility of Active Ingredients used in Plant Protection. Part III: The Temperature Relationship Between Vapour Pressure and Evaporation Rate. *Pestic. Sci.* **1982**, *13*, 161–168. [CrossRef]
36. Elder, J.P. Sublimation Measurements of Pharmaceutical Compounds by Isothermal Thermogravivletry. *J. Therm. Anal.* **1997**, *49*, 897–905. [CrossRef]
37. Yan, W.; Suppes, G.J. Vapor Pressures and Evaporation Studies of Sugars and Sugar Alcohols. *J. Chem. Eng. Data* **2008**, *53*, 2033–2040. [CrossRef]
38. Wright, S.F.; Dollimore, D.; Dunn, J.G.; Alexander, K. Determination of the Vapor Pressure Curves of Adipic Acid and Triethanolamine using Thermogravimetric Analysis. *Thermochim. Acta* **2004**, *421*, 25–30. [CrossRef]
39. Association, G.P. *Physical Properties of Glycerine and Its Solutions*; Glycerine Producers' Association: New York, NY, USA, 1963.
40. Brunetti, B.; Ciccioli, A.; Gigli, G.; Lapi, A.; Misceo, N.; Tanzi, L.; Vecchio Ciprioti, S. Vaporization of the Prototypical Ionic Liquid $BMImNTf_2$ under Equilibrium Conditions: A Multitechnique Study. *Phys. Chem. Chem. Phys.* **2014**, *16*, 15653–15661. [CrossRef] [PubMed]
41. Tokuda, H.; Ishii, K.; Susan, M.A.B.H.; Tsuzuki, S.; Hayamizu, K.; Watanabe, M. Physicochemical Properties and Structures of Room-Temperature Ionic Liquids. 3. Variation of Cationic Structures. *J. Phys. Chem. B* **2006**, *110*, 2833–2839. [CrossRef]
42. Tokuda, H.; Tsuzuki, S.; Susan, M.A.B.H.; Hayamizu, K.; Watanabe, M. How Ionic Are Room-Temperature Ionic Liquids? An Indicator of the Physicochemical Properties. *J. Phys. Chem. B* **2006**, *110*, 19593–19600. [CrossRef] [PubMed]
43. Tokuda, H.; Hayamizu, K.; Ishii, K.; Susan, M.A.B.H.; Watanabe, M. Physicochemical Properties and Structures of Room Temperature Ionic Liquids. 1. Variation of Anionic Species. *J. Phys. Chem. B* **2004**, *108*, 16593–16600. [CrossRef]
44. Lovelock, K.R.J.; Deyko, A.; Corfield, J.-A.; Gooden, P.N.; Licence, P.; Jones, R.G. Vaporisation of a Dicationic Ionic Liquid. *ChemPhysChem* **2009**, *10*, 337–340. [CrossRef]

45. Jessop, P.G.; Jessop, D.A.; Fu, D.; Phan, L. Solvatochromic Parameters for Solvents of Interest in Green Chemistry. *Green Chem.* **2012**, *14*, 1245–1259. [CrossRef]
46. Organization, I.L. The International Chemical Safety Cards Database. Available online: https://www.ilo.org/dyn/icsc/showcard.listCards3?p_lang=en (accessed on 3 January 2017).
47. Ueno, K.; Yoshida, K.; Tsuchiya, M.; Tachikawa, N.; Dokko, K.; Watanabe, M. Glyme–Lithium Salt Equimolar Molten Mixtures: Concentrated Solutions or Solvate Ionic Liquids? *J. Phys. Chem. B* **2012**, *116*, 11323–11331. [CrossRef]
48. Kelkar, M.S.; Maginn, E.J. Calculating the Enthalpy of Vaporization for Ionic Liquid Clusters. *J. Phys. Chem. B* **2007**, *111*, 9424–9427. [CrossRef]
49. Pandey, A.; Pandey, S. Solvatochromic Probe Behavior within Choline Chloride-Based Deep Eutectic Solvents: Effect of Temperature and Water. *J. Phys. Chem. B* **2014**, *118*, 14652–14661. [CrossRef]
50. Greaves, T.L.; Drummond, C.J. Protic Ionic Liquids: Properties and Applications. *Chem. Rev.* **2008**, *108*, 206–237. [CrossRef]
51. MacFarlane, D.R.; Tachikawa, N.; Forsyth, M.; Pringle, J.M.; Howlett, P.C.; Elliott, G.D.; Davis, J.H.; Watanabe, M.; Simon, P.; Angell, C.A. Energy Applications of Ionic Liquids. *Energy Environ. Sci.* **2014**, *7*, 232–250. [CrossRef]
52. Emel'yanenko, V.N.; Boeck, G.; Verevkin, S.P.; Ludwig, R. Volatile Times for the Very First Ionic Liquid: Understanding the Vapor Pressures and Enthalpies of Vaporization of Ethylammonium Nitrate. *Chem. Eur. J.* **2014**, *20*, 11594. [CrossRef]
53. Capelo, S.B.; Méndez-Morales, T.; Carrete, J.; López Lago, E.; Vila, J.; Cabeza, O.; Rodríguez, J.R.; Turmine, M.; Varela, L.M. Effect of Temperature and Cationic Chain Length on the Physical Properties of Ammonium Nitrate-Based Protic Ionic Liquids. *J. Phys. Chem. B* **2012**, *116*, 11302–11312. [CrossRef] [PubMed]